Maxwell-Hall access resistance in graphene nanopores – Supplementary Information

Subin Sahu[1,2,3] and Michael Zwolak[1,*]

[1] *Center for Nanoscale Science and Technology, National Institute of Standards and Technology, Gaithersburg, MD 20899, USA*

[2] *Maryland NanoCenter, University of Maryland, College Park, MD 20742, USA*

[3] *Department of Physics, Oregon State University, Corvallis, OR 97331, USA*

CONTENTS

* mpz@nist.gov

I. METHODS

A. All-atom MD simulations

Our system consists of a single-layer graphene membrane with a pore in the center and in 1 Mol/L KCl solution, as shown in Figure 1 of the main text. We build the system using VMD 1.9.1 [1] and perform all-atom molecular dynamics simulations using NAMD2 [2] with periodic boundary condition in all directions. The force field parameters are rigid TIP3P [3] for water and CHARMM27 [4] for the other atoms. We fix the outer edge of the graphene membrane but the bulk of the membrane has no confinement other than the C-C bonds of graphene. The simulations have an integration time step of 2 fs and Langevin damping of 0.2 ps for only carbon and water (via its oxygen atoms). Non-bonded interactions (van der Waals and electrostatics) have a cutoff of 1.2 nm. However, full electrostatic calculations occur every 4 time steps using the Particle Mesh Ewald (PME) method. We first minimize the energy of the system for 4000 steps (8 ps) and then heat it to 295 K in another 8 ps. A 1 ns NPT (constant number of particles, pressure and temperature) equilibration using the Nose-Hoover Langevin piston method [5] – to raise the pressure to 101 325 Pa (i.e., 1 atm) – followed by 3 ns of NVT (constant number of particles, volume and temperature) equilibration generates the initial atomic configuration. An electric field perpendicular to the plane of the membrane (1 V potential difference) drives the ionic current through the pore.

B. Pore radius

We consider three pore sizes with effective radius $a = 0.49$ nm, $a = 1.18$ nm, and $a = 1.81$ nm, as shown in Figure S-1. Geometrically, the radius of the pore can be defined as the average distance between the center of the pore and the pore atoms at the edge minus the van der Waals radius of carbon (0.17 nm), i.e., the average distance between the center of pore and edge of the carbon atoms. However, the radius of the accessible area for the transport of ions is about 0.2 nm smaller than r_p, as shown in Figure S-2. The exclusion near the pore edge is due to van der Waals (vdW) repulsion (i.e., the finite ion size since we already account for carbon's vdW radius) and dehydration. Thus, we define the effective

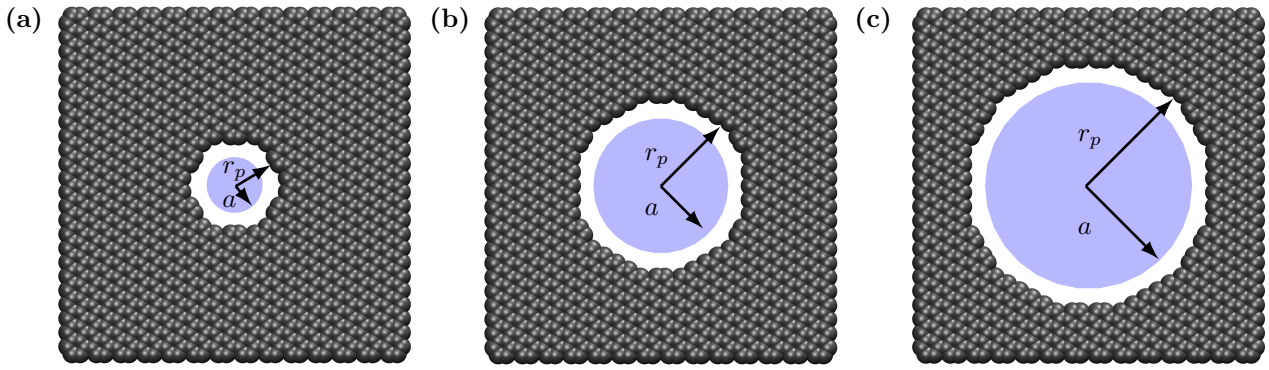

FIG. S-1. A 6 nm × 6 nm section of the graphene sheet showing the pores with effective radii (a) $a = 0.49$ nm, (b) $a = 1.18$ nm, and (c) $a = 1.81$ nm. We construct the pores by removing all carbon atoms within 0.8 nm, 1.5 nm, and 2.2 nm, respectively, of the pore center and also removing any dangling bonds. The geometric definition of the pore radius, r_p, is the average distance between the center of the pore and the inner edge of the pore atoms (i.e., carbons with a size given by their vdW radius). However, the effective pore radius, a, is about 0.2 nm smaller than r_p due to the finite size (hydration and vdW radii) of the ions. The schematic view here is in agreement with the statistical view of ion crossings, see Figure S-2, with the exception of some minor contextual issues arising from the pore atomic structure (e.g., the ion crossings have a clear hexagonal symmetry).

radius, a of the pore as

$$\pi a^2 \bar{J} = \int_0^{r_p} J(\rho) 2\pi\rho d\rho, \tag{1}$$

where $J(\rho)$ is the current density at radial coordinate ρ (assuming cylindrical symmetry, which is reasonable for graphene pores but not perfect – relaxing this would require much longer simulations to acquire sufficient statistics on the angular dependence of ion crossings) and $\bar{J}$ is the average current density in the region of the pore where $J(\rho)$ is flat. This calculation is essentially weighing the area contributions by the Boltzmann factors at that location, except we use the out-of-equilibrium probability distribution of ion crossing events instead of the Boltzmann factors from the free energy barriers. The quantity $\bar{J}$ serves the role of an "unattenuated" current density – i.e., the current density where there is no excess free energy barrier. We note that fluctuations of the graphene membrane, specifically around the pore edge, also affects the pore size and its effect is included in Eq. (1).

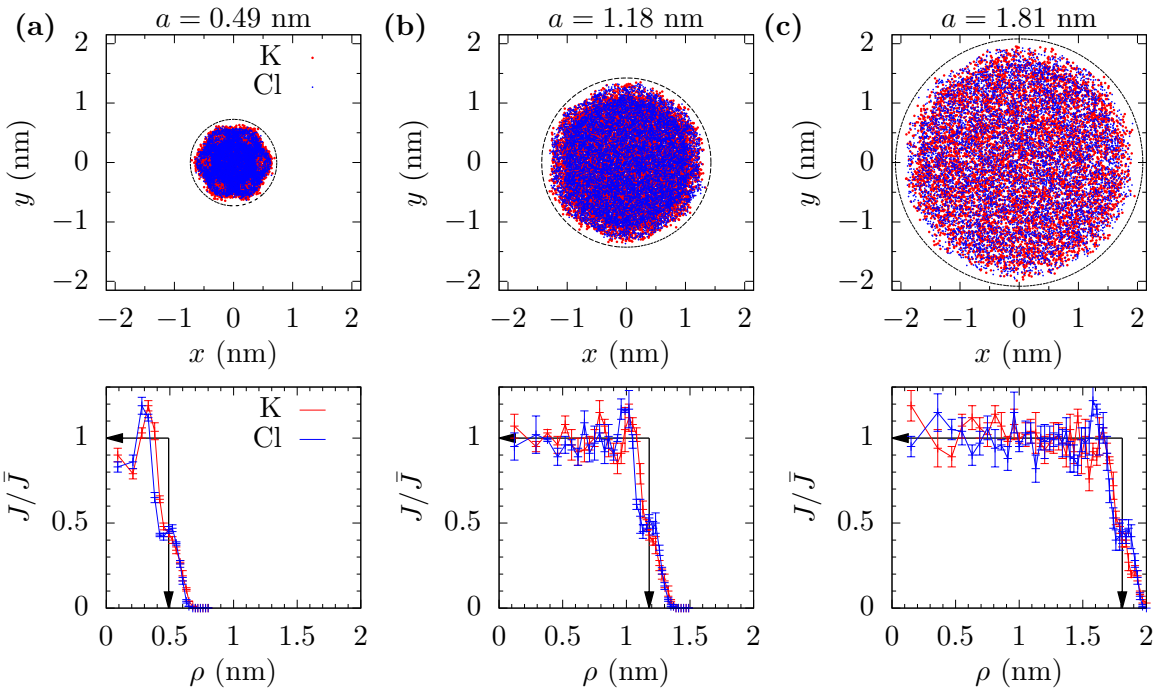

FIG. S-2. Current density of K^+ and Cl^- crossing pores with radii (a) $a = 0.49$ nm, (b) $a = 1.18$ nm, and (c) $a = 1.81$ versus the cylindrical coordinate $\rho = \sqrt{x^2 + y^2}$. The top panels show scatter plots of ion crossings in the xy-plane. The circles indicate r_p – the geometric pore radius – which is about 0.2 nm bigger than the radius of the accessible area, as seen by the gap in the ion crossing events. The bottom panels show variation of current density J, normalized by "unattenuated" current density $\bar{J}$, with radial coordinate ρ inside the pore. The black arrows show the effective pore radius from this distribution of J. Error bars are ± 1 standard error from six parallel simulations.

C. Error analysis for convergence in time

We compute the error in the MD results using the block standard error (BSE) method [6]. We divide a single MD run of duration T into number of contiguous blocks of equal duration τ. The BSE is given by

$$\text{BSE} = \frac{s_\tau \sqrt{\tau}}{\sqrt{T}}, \tag{2}$$

where $s_\tau = \sqrt{\frac{\sum_i (\langle I_\tau \rangle_i - \langle I_T \rangle)^2}{(N_b - 1)}}$ is the standard deviation of the mean current $\langle I_\tau \rangle$, within each of the N_b blocks. The error bars in the plots are ± 1 BSE unless otherwise noted.

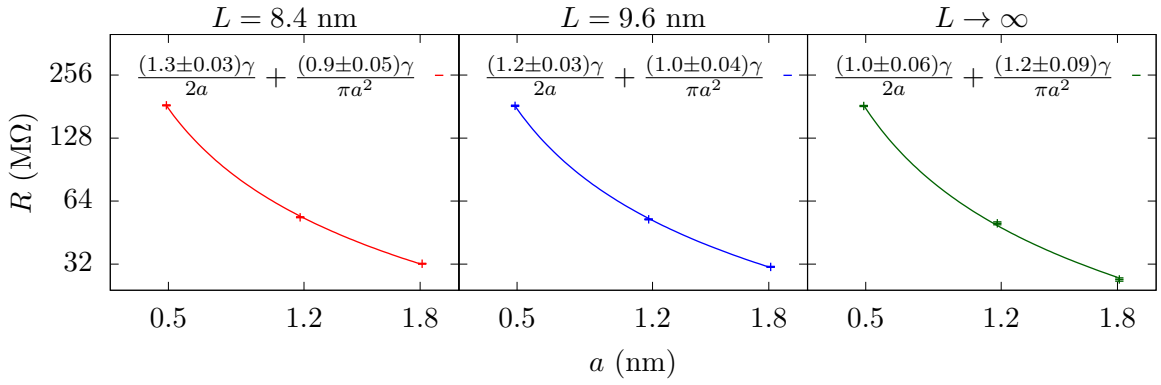

FIG. S-3. Maxwell-Hall form of the access resistance fitted for $L = 8.4$ nm, $L = 9.6$ nm, and $L \to \infty$ (extrapolated resistance). Only when $L \to \infty$ does the exact Maxwell-Hall form emerge for the access resistance, i.e., a coefficient of 1 times $\gamma/2a$. The error bars are ± 1 BSE.

II. FINITE-SIZE SCALING

As mentioned in the main text, if all the linear dimensions of the cell (experimental or theoretical) are simultaneously taken to be large, the normal bulk component of the resistance will vanish and the measured resistance is expected to take on the form

$$R_\infty = \frac{\gamma}{2a} + \frac{\gamma h_p}{\pi a^2} \tag{3}$$

in the continuum limit and assuming a cylindrical pore of height h_p. R_∞ can be found by using the finite-size scaling

$$R = \gamma \left(\frac{H}{\mathcal{G}L^2} - \frac{f}{\mathcal{G}L} \right) + R_\infty, \tag{4}$$

where $\mathcal{G}L^2$ is the cross-sectional area of the cell, L is the cross-sectional length, $\mathcal{G}$ is a geometric factor ($\mathcal{G} = \pi/4$ for a cylindrical cell and $\mathcal{G} = 1$ for a rectangular cell), and f is the fitting parameter.

In Figure S-3, we fit a modified form of Eq. 3 for $L = 8.4$ nm, $L = 9.6$ nm, and $L \to \infty$,

$$R_L = \frac{b_L \gamma}{2a} + \frac{h_L \gamma}{\pi a^2}, \tag{5}$$

where b_L and h_L are the fitting parameters. For $L = 8.4$ nm and $L = 9.6$ nm, the access resistance is larger than the Maxwell-Hall form due to the unbalanced dimensions of the cell and the cell's relative size compared to the differing pore radii. Only when $L \to \infty$ do we get exactly the Maxwell-Hall value. Also, the fitted value of the membrane thickness is ≈ 1.2 nm. This is consistent with the separation of ion density peak on the two sides of the graphene membrane (i.e., the charge dipole layer separation), as seen in Figure S-4.

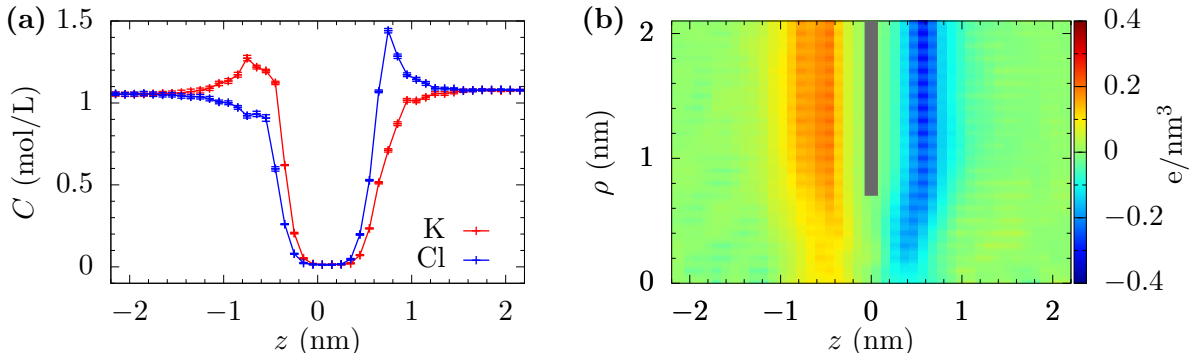

FIG. S-4. (a) K^+ and Cl^- ion densities, and (b) net charge density when a 1 V voltage is applied across a graphene membrane with a radius $a = 0.49$ nm pore. The peak of K^+ ion concentration is closer to the graphene membrane than that of Cl^- due to smaller ionic size of the former. The z distance between the two peaks is about 1.5 nm. The error bars are ± 1 standard error from six parallel simulations.

III. ELECTRIC FIELDS AND CURRENT DENSITY

We calculate the electrostatic potential and the charge density using the VolMap plugin of VMD. The current density is the average ion displacement between the snapshots (10 ps) over the length of the simulation,

$$\vec{J}(\vec{r}) = \frac{\sum_i q_i \vec{v}_i(\vec{r})}{dV}, \tag{6}$$

where the sum is over all the ions within the volume element dV(with $dx = dy = dz = 0.1$ nm) at position $\vec{r}$.

Figure S-5 shows the flow pattern for three different cell cross sections with a pore radius $a = 1.18$ nm. In each of them, the current density J quickly orients along z-axis. It is also seen from Fig S-5 that J decreases with $A = \mathcal{G}L^2$, which can be understood by looking at the average value of J_z according to our model,

$$\langle J_z \rangle = \frac{V}{RA} = \frac{V}{\gamma(H - fL) + R_\infty \mathcal{G}L^2}. \tag{7}$$

IV. BULK RESISTIVITY

We calculate the bulk resistivity from our MD simulations using a cell without the graphene membrane/pore. The standard value of the bulk resistivity is $\gamma = 1/ne(\mu_K + \mu_{Cl}) \approx$

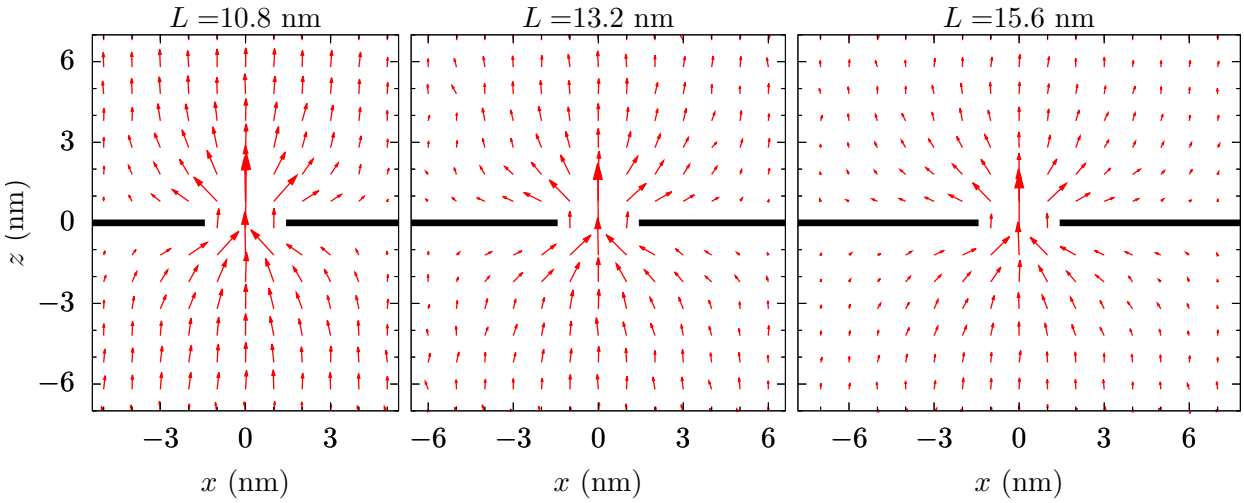

FIG. S-5. The current density, J, showing the flow pattern for different cell cross sections from MD simulations of a graphene nanopore with radius $a = 1.18$ nm. The flow quickly orients with the z-axis away from the pore regardless of the cross-sectional area of the cell. Note that J is not constant with L due to a changing balance of bulk and pore resistance.

67 MΩ·nm. The value from MD is $\gamma_{\mathrm{MD}} \approx 70$ MΩ·nm, as shown in Figure S-6. It is to be noted that the actual value of resistivity of 1 M KCl at room temperature observed in experiments is $\gamma_{\mathrm{exp}} \approx 90$ MΩ·nm. At the high concentration of KCl (such as 1 mol/L), the conductance deviates from the linear expression, $\gamma = 1/ne(\mu_{\mathrm{K}} + \mu_{\mathrm{Cl}})$. However, the MD results give the conductance according to the linear expression.

In Figure S-7 we plot the potential drop along the z-direction when 1 V potential is applied across the graphene membrane. At larger distances, Δz, from the pore, the potential drop, ΔV, is proportional to the bulk resistivity γ, since

$$\Delta V = I\Delta R = \frac{I\gamma\,\Delta z}{A}, \tag{8}$$

where ΔR is the resistance of the region away from the pore.

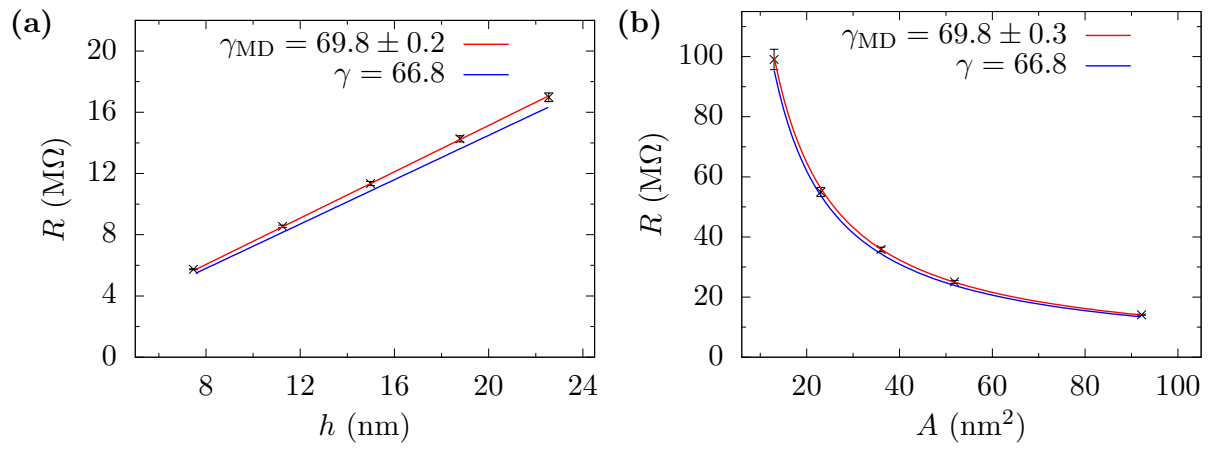

FIG. S-6. (a) Resistance versus simulation cell height and (b) resistance versus cross-sectional area for a bulk solution of 1 mol/L KCl. The red line gives γ_{MD} as the best fit to $R = \gamma_{MD} h/A$, and the blue line shows standard resistivity $\gamma = 1/ne\,(\mu_K + \mu_{Cl}) \approx 67$ MΩ·nm. The error bars are ±1 BSE.

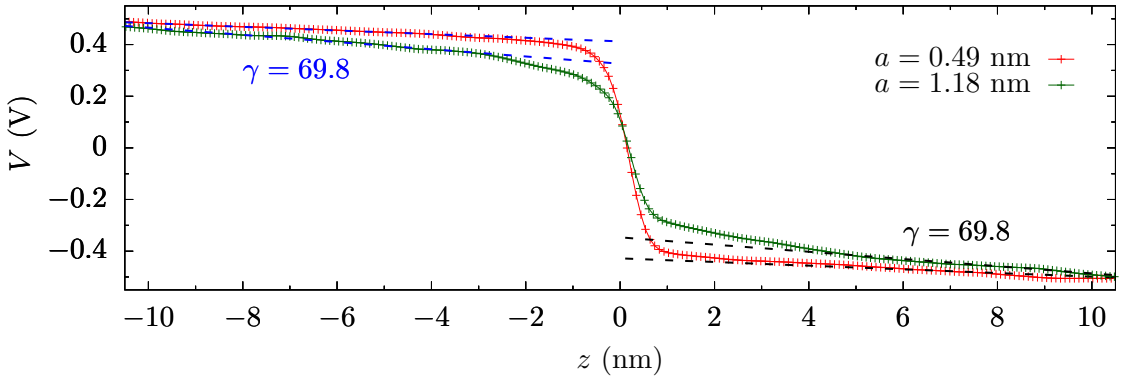

FIG. S-7. Potential V versus the z-distance averaged over a cylindrical region of radius $\rho = 1$ nm for $a = 0.49$ nm (red line) and radius $\rho = 2$ nm for $a = 1.18$ nm (green line). The slope of potential drop is constant and equal to bulk resistiviy beyond $|z| \gtrsim L/2$ (with $L = 9.6$ for $a = 1.18$ nm and $L = 7.2$ nm for $a = 0.49$ nm). But within $|z| \lesssim L/2$ the slope increases initially very slowly and then very rapidly near the pore ($z = 0$). The error in the potential is comparable to the size of data markers.

[1] W. Humphrey, A. Dalke, and K. Schulten, J. Mol. Graphics **14**, 33 (1996).

[2] J. C. Phillips, R. Braun, W. Wang, J. Gumbart, E. Tajkhorshid, E. Villa, C. Chipot, R. D. Skeel, L. Kale, and K. Schulten, J. Comput. Chem. **26**, 1781 (2005).

[3] W. L. Jorgensen, J. Chandrasekhar, J. D. Madura, R. W. Impey, and M. L. Klein, J. Chem. Phys. **79**, 926 (1983).

[4] S. E. Feller and A. D. MacKerell, J. Phys. Chem. B **104**, 7510 (2000).

[5] G. J. Martyna, D. J. Tobias, and M. L. Klein, J. Chem. Phys. **101**, 4177 (1994).

[6] A. Grossfield and D. M. Zuckerman, Annu. Rep. Comput. Chem. **5**, 23 (2009).